Physics Letters A 376 (2012) 1812–1817

Contents lists available at SciVerse ScienceDirect

Physics Letters A

www.elsevier.com/locate/pla

The interaction between quantum dots and coupled magnetic plasmon in coupled metamaterial

S.M. Wang [a,*], H. Liu [a], T. Li [a], S.N. Zhu [a], X. Zhang [b]

[a] National Laboratory of Solid State Microstructures and Department of Physics, Nanjing University, Nanjing 210093, China
[b] Nanoscale Science and Engineering Center, 5130 Etcheverry Hall, University of California, Berkeley, CA 94720-1740, United States

ARTICLE INFO

Article history:
Received 16 December 2011
Received in revised form 23 March 2012
Accepted 8 April 2012
Available online 11 April 2012
Communicated by R. Wu

Keywords:
Metamaterial
Stimulated emission
Quantum optics

ABSTRACT

The coupled magnetic plasmons (CMPs) has been investigated in an active system composed of coupled metamaterial and quantum dots. By introducing a full-quantum description of CMPs, the interaction Hamiltonian of the active system was obtained, through which the stimulated emission could be investigated. The results showed that the CMP amplification by the stimulated emission radiation could be achieved under certain conditions. This may be used to work as a CMP source in the integrated optics and nano-photonics.

1. Introduction

As a new type of artificial material, plasmonic metamaterials are not composed of natural atoms or molecules, but of micro-metallic/nano-metallic LC circuit resonators (also called meta-atoms or meta-molecules) [1–4]. When light interacts with metamaterials, oscillating currents will be induced in these LC resonators, leading to a strong magnetic plasmon resonance [1]. Therefore, high-frequency magnetism, which does not exist in natural materials, is obtained. It has been theoretically and experimentally confirmed that the dispersion of this medium strongly depends on the frequency of light, and that electric and magnetic fields are highly confined to subwavelength scales as the frequency of light obtains access to the resonance region of these LC resonators. Negative refraction and superlensing [5], cloaking [6,7], and EIT (electromagnetically induced transparency) effect [4] all occur within such a frequency region, which leads to the world-wide attention paid to metamaterials.

In most of reported works up to now, the coupling interaction between meta-atoms are ignored and the effective properties of metamaterials can be seen as average effect of many single plasmonic resonators. However, in practical metamaterials, the coupling effect between meta-atoms should always exist, which is significant when the distance between resonators is small [8,9]. After including coupling effect, the properties of metamaterials are quite different and complicated, which can be seen as a kind of "meta-solid". Similar to conventional solid-state matter, the concept of excitation has to be introduced to coupled metamaterials in accordance with the concepts of solid-state physics and quantum physics [10,11].

Moreover, since the first demonstration of the plasmon-assisted entangled photons in perforated metal film has been reported, the quantum characteristics in plasmonic system and metamaterials have been continuously reported and have attracted more and more study interest for their potential applications in quantum information techniques [12–15]. Recently, the quantum generator made from SPASER (surface plasmon amplification by stimulated emission of radiation) system has also been introduced, in which a generalized quantum treatment of surface plasmon has been introduced using the spectral representation method [12]. All these improvement require a profound understanding of the fundamental quantum properties of coupled metamaterials. Therefore, one can go forward to further study the interaction between coupled metamaterials and other materials.

In this work, we investigate the interaction between quantum dots and a one-dimensional coupled metamaterial composed of a chain of nanosandwiches. The linear properties of the nanosandwich chain are presented in Section 2. A full quantum treatment of the coupled metamaterial is introduced in Section 3. According to this, the interaction Hamiltonian of the compound system composed by a chain of nanosandwiches and the PbS quantum dot is achieved and the stimulated emission is investigated in Section 4. At last, the conclusion is presented in Section 5.

* Corresponding author. Tel.: +86 25 83621239; fax: +86 25 83595535.
E-mail address: wangshuming@nju.edu.cn (S.M. Wang).
URL: http://dsl.nju.edu.cn/dslweb/images/plasmonics-MPP.htm (S.M. Wang).

0375-9601/$ – see front matter
http://dx.doi.org/10.1016/j.physleta.2012.04.016

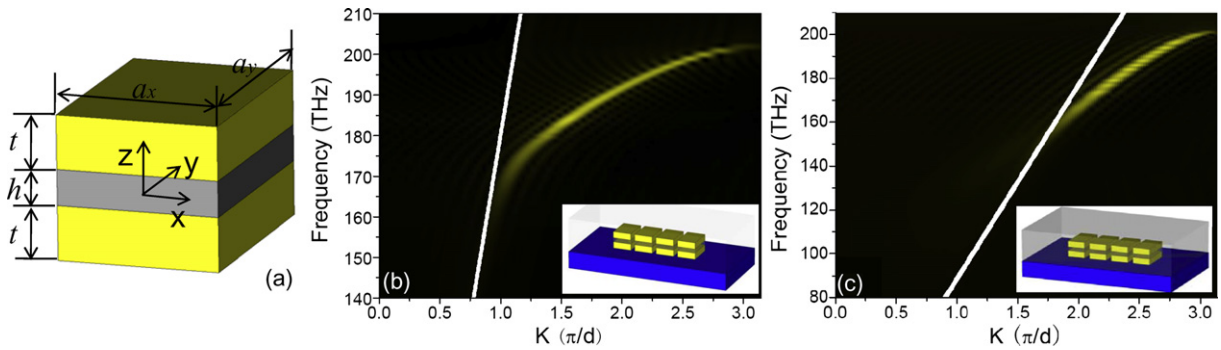

Fig. 1. The geometry of a single nanosandwich is shown in (a). The Fourier transformation maps, with $a_x = 215$ nm, $a_y = 300$ m, $t = 75$ nm and $h = 50$ nm in Case I and $a_x = 160$ nm, $a_y = 300$ m, $t = 75$ nm, and $h = 50$ nm in Case II are shown in (b) and (c), respectively. In both cases, $\Delta = d - a_x = 50$ nm and the white lines corresponds to the light line. The sketches of the two cases are presented in the insets, respectively in (b) and (c).

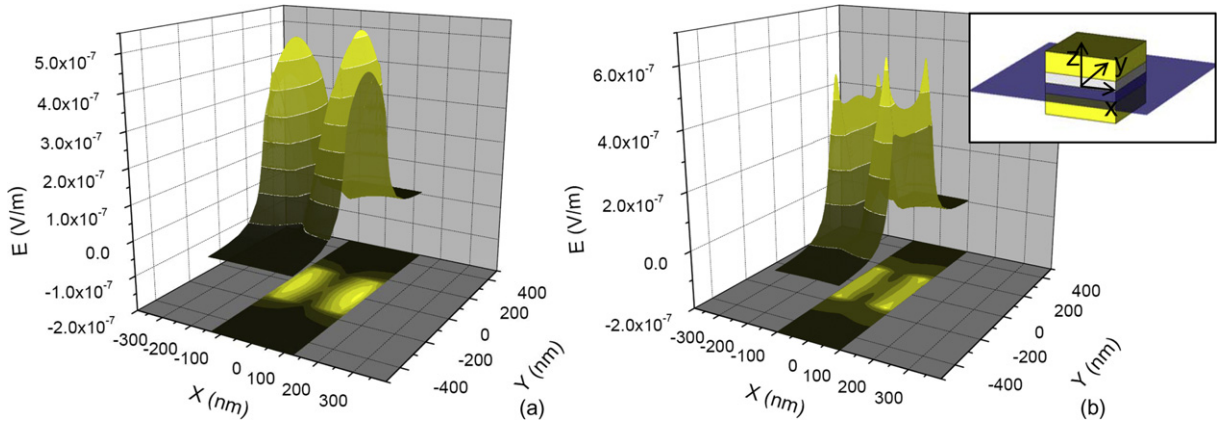

Fig. 2. The normalized electric field distribution on the $z = 0$ plane of the nanosandwich in Case I and Case II are respectively shown in (a) and (b), at telecom wavelength. An inset illustrates the position of the $z = 0$ plane (blue plane) in the nanosandwich. (For interpretation of the references to color in this figure legend, the reader is referred to the web version of this Letter.)

2. Coupled metamaterial composed of a nanosandwich chain

Among the variety of structures able to produce magnetic resonance, nanosandwich structure is a good choice to obtain high frequency magnetism even in light region with a simple structure for fabrication convenience. Many important properties of metamaterials in light region were realized from such structure [16]. In this work, the nanosandwiches are closely placed in a line to form a one-dimensional coupled metamaterial. The geometry of a single nanosandwich is depicted in Fig. 1a. The metallic component is silver with a Drude-type electric permittivity $\varepsilon_{silver} = 1 - \omega_p^2/(\omega^2 + i\omega\gamma)$, where $\omega_p = 1.37 \times 10^{16}$ s^{-1} and $\gamma_m = 12.24 \times 10^{13}$ s^{-1} [8]. The nanosandwich is placed on a silica substrate. When the middle layer of the nanosandwich is filled with a non-metallic material, the magnetic resonance can be formed by the excited magnetic loop composed of currents in the two separated metal layers and the displacement currents in the outside surrounding [17]. The electromagnetic field is highly confined in the middle layer. Here, the middle layer of the nanosandwich is filled with the active material, semiconductor PbS quantum dot material, with the emission wavelength of approximately 1550 nm, telecom wavelength, and the electric permittivity $\varepsilon_{\mathrm{PbS}} = 23$. The quantum dots are densely packed in vacuum in the middle layer [12].

In the coupled metamaterial, the magnetic resonances in nanosandwiches couple with each other and form a CMP, a collective magnetic resonance throughout the chain [8,17]. Two cases of the coupled metamaterials are studied: the one-dimensional coupled metamaterial embedded in vacuum (Case I) and embedded in quantum dot material (Case II). The field distribution of the system can be calculated by using the commercial software package CST MICROWAVE STUDIO. Moreover, a Fourier transformation (FT) method, $H(\omega, k) = \int H(\omega, x)e^{ikx}\,dx$, is also employed to analyze the linear condition or the low pumping power condition of the system, where the nonlinear properties or the interaction between metamaterial and quantum dot material can be neglected. Since the magnetic filed in the nanosandwiches reaches the peaks in the middle line of the chain, we can just do the FT process on the magnetic field along this line to directly observe the excited CMP mode in such one-dimensional coupled metamaterial through the strength of the magnetic field after doing an FT process [17]. In Figs. 1b and 1c, an evident CMP mode band can be observed in both cases, below the light line (white line). Since these strong CMP modes are located below the light line, they are the extended modes along the chain, which cannot leak to the outside space for the mismatching of the wave vector. Therefore, these CMP modes are quite strong, resulting in a high interaction with the active materials. To keep the strong CMP modes around the emission frequency of the PbS quantum dot material, telecom frequency, the geometry parameters of the one-dimensional coupled metamaterials is carefully designed in both cases. The electric field distribution in the nanosandwiches is also investigated for the electric field plays the most important role in the interaction with the quantum dots, which can be regarded as electric dipoles. The electric field distribution is numerically calculated at the telecom wavelength and plotted in Fig. 2 for both cases. For the smaller size of the nanosandwich in Case II, the field in it is pushed to its edges, and somewhat quadrupole effect can be found, leading to the more peaked and non-uniformly distributed than the electric field distribution in Case I. The high-magnitude areas of the electric field, which is tightly closed to the magnetic field hot spots in

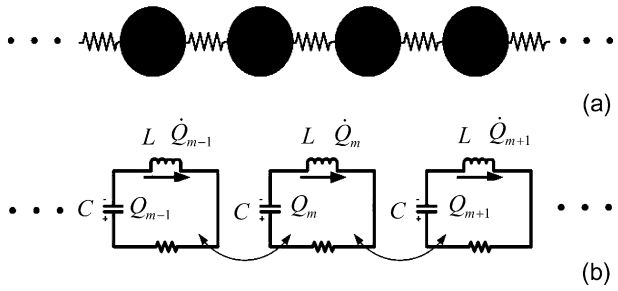

Fig. 3. (a) Model of coupled metamaterial; (b) Equivalent LC circuit model.

the nanosandwiches, correspond to the strong interaction between the coupled metamaterial and the quantum dots.

On the other hand, a theoretical treatment based on the Lagrangian equations can also be employed to investigate the coupled metamaterial [8]. The resonators in the coupled metamaterial can be seen as LC circuits [2]. The theoretical model and equivalent LC circuit model of the coupled metamaterial are shown in Figs. 3a and 3b, by considering only the nearest-neighbor coupling. The Lagrangian of the nanosandwich chain is expressed as follows based on Fig. 3b [8],

$$\mathcal{L} = \sum_m \left[\frac{L}{2}\dot{Q}_m^2 - \frac{1}{2C}Q_m^2 + \frac{M_h}{2}(\dot{Q}_m\dot{Q}_{m+1} + \dot{Q}_m\dot{Q}_{m-1}) - \frac{M_e}{2}(Q_mQ_{m+1} + Q_mQ_{m-1}) \right]. \quad (1)$$

In this equation, m represents the mth unit cells; L and C are the inductor and the capacity of the single resonator, respectively; and M_h and M_e describe the magnetic and electric coupling between the unit cells, respectively. Here, Q_m and $\dot{Q}_m$ correspond to the charge and current on the mth unit cell, respectively. The terms formed by $\dot{Q}$ are the current-induced kinetic energies, and those consisting of Q denote the charge-induced potential energy. By using the Lagrangian equations $\frac{d}{dt}(\frac{\partial \mathcal{L}}{\partial \dot{Q}_m}) - \frac{\partial \mathcal{L}}{\partial Q_m} = 0$, we finally obtain the dispersion relation of the new excitation in the coupled metamaterial as follows:

$$\omega(k) = \omega_0\sqrt{\frac{1+\kappa_e\cos(kd)}{1+\kappa_h\cos(kd)}}, \quad (2)$$

where $\omega_0^2 = 2\pi/LC$ is the resonant frequency of the unit cell itself and $\kappa_h = 2M_h/L$ and $\kappa_e = 2M_eC$ are the magnetic and electric coupling coefficient, respectively [8].

According to the dispersion relation in Eq. (2), we can obtain the coupling coefficients as $\kappa_h = 0.28$ and $\kappa_e = 0.55$ in Case I, and $\kappa_h = 0.04$ and $\kappa_e = 0.77$ in Case II [8].[1] In Figs. 4a and 4b, the theoretical results based on Lagrangian (red line) are consistent with the simulation results (blue dots), confirming the correctness of our processing method. Moreover, the couplings in these systems, both the magnetic and electric couplings, strongly depend on the spacing between nanosandwiches, d. Generally, a smaller distance between resonators will produce stronger coupling, thus leads to the decline property of the coupling coefficients with the increasing of the spacing, see Figs. 4c and 4d. For the smaller length of a_x, the electric field will leak more to the outside space. Therefore, the electric field in Case II shows better confinement than that in Case I, leading to a stronger electric coupling between the nanosandwiches, as well as a broader band.

[1] Because the coupling will increase the charge and current of a nanosandwich compared with single nanosandwich, L and C will also enlarge. Therefore, in the calculation of dispersion relation, we need to introduce certain modification on ω_0 by a factor about 90–95%.

3. Quantum description of coupled metamaterial

To investigate the interaction between the CMP in one-dimensional metamaterial and quantum dots, we use a full quantum treatment based on the quantization on the Hamiltonian of the CMP, which can be considered as a kind of excitation in the artificial material [10,11]. By using a Legendre transformation, $\mathcal{H} = \sum_m P_m\dot{Q}_m - \mathcal{L}$, we can obtain the Hamiltonian of the coupled metamaterial that plays a much more important role than the Lagrangian in solid-state physics. With the generalized momentum $P_m = \partial\mathcal{L}/\partial\dot{Q}_m$ correlated with Q_m, the Hamiltonian can be expressed as follows:

$$\mathcal{H}(Q_m,\dot{Q}_m) = \sum_m \left[\frac{L}{2}\dot{Q}_m^2 + \frac{1}{2C}Q_m^2 + \frac{M_h}{2}(\dot{Q}_m\dot{Q}_{m+1} + \dot{Q}_m\dot{Q}_{m-1}) + \frac{M_e}{2}(Q_mQ_{m+1} + Q_mQ_{m-1}) \right]. \quad (3)$$

We carried out a Fourier transformation to this Hamiltonian and obtained the following expression:

$$\mathcal{H}(Q_{\boldsymbol{k}},\dot{Q}_{-\boldsymbol{k}}) = \sum_{\boldsymbol{k}} \left[\frac{L}{2}\dot{Q}_{\boldsymbol{k}}\dot{Q}_{-\boldsymbol{k}} + M_h\cos(kd)\dot{Q}_{\boldsymbol{k}}\dot{Q}_{-\boldsymbol{k}} + \frac{1}{2C}Q_{\boldsymbol{k}}Q_{-\boldsymbol{k}} + M_e\cos(kd)Q_{\boldsymbol{k}}Q_{-\boldsymbol{k}} \right], \quad (4)$$

where d refers to the period of the metamaterial, and the Fourier expansion $Q_m = \frac{1}{\sqrt{M}}\sum_{\boldsymbol{k}} Q_{\boldsymbol{k}}e^{i\boldsymbol{k}\boldsymbol{R}_m}$ is used. Charge $Q_{\boldsymbol{k}}$ has a canonically conjugate variable $P_{\boldsymbol{k}} = \partial\mathcal{L}/\partial\dot{Q}_{\boldsymbol{k}} = (\frac{L}{2} + M_h\cos(kd))\dot{Q}_{-\boldsymbol{k}}$. As seen in Figs. 4a and 4b, the system has the lowest energy at the Brillouin zone center ($kd = 0$) and the highest energy at the edge of the Brillouin zone ($kd = \pi$). Therefore, according to the Hamiltonian in Eq. (4), M_h and M_e should both be positive, consistent with the results that we obtained above.

Considering the quantum condition, $\hat{Q}_m$ and $\hat{P}_m$ possess the commutation relation $[\hat{Q}_m,\hat{P}_m] = i\hbar$ [18,19]. After some derivation, the commutator between $\hat{Q}_{\boldsymbol{k}}$ and $\hat{P}_{\boldsymbol{k}}$ can also be derived as $[\hat{Q}_{\boldsymbol{k}},\hat{P}_{\boldsymbol{k}}] = i\hbar$. In the derivation, the unitary condition $\frac{1}{M}\sum_m e^{i(\boldsymbol{k}+\boldsymbol{k}')md} = \delta_{\boldsymbol{k},-\boldsymbol{k}}$ is used. A Bogoliubov transformation has been performed to the Hamiltonian in Eq. (3) by introducing a set of creation and annihilation operators, $\hat{a}_{\boldsymbol{k}} = U_{\boldsymbol{k}}\hat{Q}_{\boldsymbol{k}} + iV_{\boldsymbol{k}}\hat{P}_{-\boldsymbol{k}}$ and $\hat{a}^+_{\boldsymbol{k}} = U_{\boldsymbol{k}}\hat{Q}_{-\boldsymbol{k}} - iV_{\boldsymbol{k}}\hat{P}_{\boldsymbol{k}}$, with parameters $U_{\boldsymbol{k}} = (\hbar)^{-1/2}\sqrt{\xi}$ and $V_{\boldsymbol{k}} = (\hbar)^{-1/2}/\sqrt{\xi}$, and $\xi = \sqrt{[\frac{1}{2C} + M_e\cos(kd)][\frac{L}{2} + M_h\cos(kd)]}$ [18,19]. Finally, the Hamiltonian of a coupled metamaterial in number representation can be obtained as follows:

$$\hat{\mathcal{H}} = \sum_{\boldsymbol{k}} \left(\hat{a}^+_{\boldsymbol{k}}\hat{a}_{\boldsymbol{k}} + \frac{1}{2} \right)\hbar\omega_{\boldsymbol{k}}. \quad (5)$$

In the equation, we obtained the quantum description of the excitation in a coupled metamaterial. For the convenience of understanding, the concept of 'quasi-particle' can be used here to give an institutive picture of quantum property of the excitation, CMP, in such 'meta-solid'. $\hat{a}^+_{\boldsymbol{k}}$ and $\hat{a}_{\boldsymbol{k}}$ are the creating and annihilating operators, indicating the creation and destruction of 'quasi-particle', respectively, with momentum $\hbar\boldsymbol{k}$ in the coupled metamaterial, and $\hat{a}^+_{\boldsymbol{k}}\hat{a}_{\boldsymbol{k}}$ is number operator. The 'quasi-particle' describes the collective resonance behavior of the CMP throughout the entire solid-state-like metamaterial when the coupling between unit cells exists. Once the coupling shrinks to zero, the metamaterial will return to the free-gas case, in which the model will simply correspond to the excitation of the unit cell itself. Such quantum treatment can also be used in plasmonic structures composed

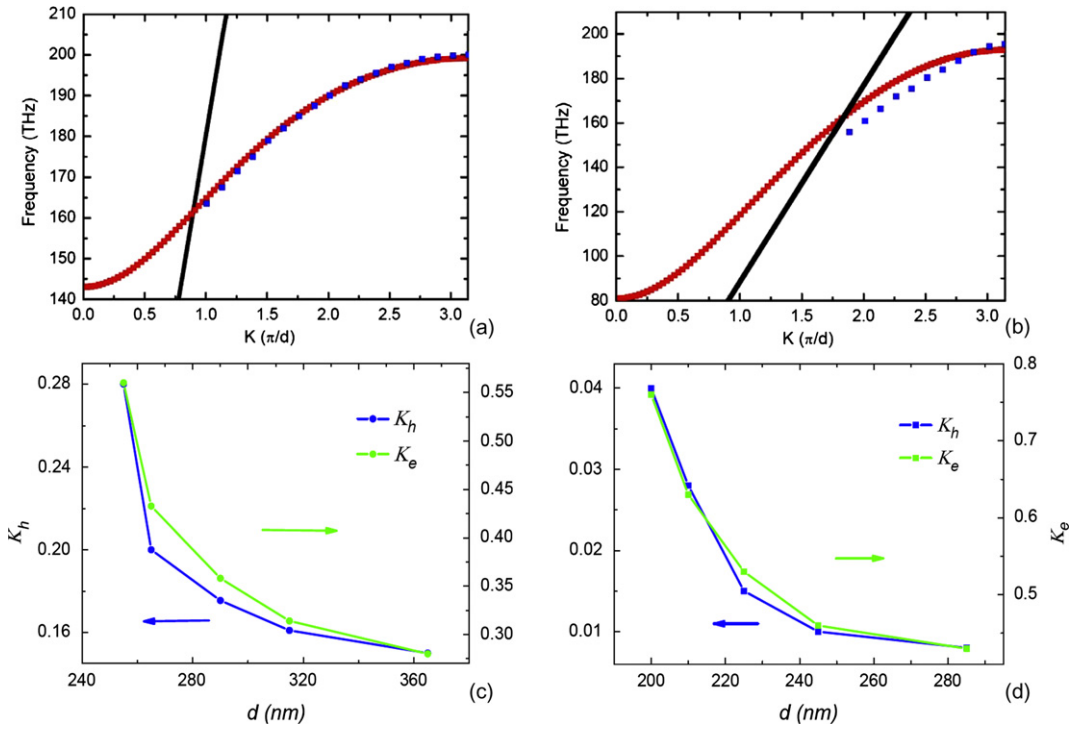

Fig. 4. The theoretical results of the dispersion relations of the CMP modes are shown in (a) and (b), respectively, in which the red line and blue dot line correspond to theoretical result and FT result, and the black line is the light line. The coupling coefficients depending on d, in Case I and Case II are shown in (c) and (d). (For interpretation of the references to color in this figure legend, the reader is referred to the web version of this Letter.)

from metallic nanostructures. A possible experimental proof of the quantum characteristic of metamaterials can be obtained through measuring the second-order quantum coherence function $g^{(2)(0)}$ in an attenuated-reflection set-up. For a quantum state, $|n\rangle$, $g^{(2)}(0) = 1 - 1/n < 1$ indicates a quantum property which can be measured directly in a practical experiment [20].

4. Interaction between quantum dot material and coupled nanosandwich chain

After introducing the Hamiltonian and the full quantum treatment of the coupled metamaterial, we can obtain the interaction Hamiltonian of the active system. The interaction Hamiltonian of the system is expressed as $\mathcal{H}_{Int} = \sum_{\boldsymbol{r}} \boldsymbol{E} \cdot \boldsymbol{d}$, where $\boldsymbol{E}$ denotes the electric field in metamaterial, $\boldsymbol{d}$ refers to the dipole moment of exciton in the quantum dot, and the summation corresponds to all quantum dots in the system [21]. After some derivation, the quantized interaction Hamiltonian can be obtained as follows (see Appendix A):

$$\hat{\mathcal{H}}_{Int} = \hbar \sum_{\boldsymbol{k}} \left[\mathbf{G}_{\boldsymbol{k}} \left(\hat{a}_{\boldsymbol{k}}^{+} \hat{\sigma}_{\boldsymbol{k}}^{-} + \hat{a}_{\boldsymbol{k}} \hat{\sigma}_{\boldsymbol{k}}^{+} \right) \right]. \tag{6}$$

Here, the coupling constant $\mathbf{G}_{\boldsymbol{k}}$ is equal to

$$\sqrt{\int \left(\rho_2(\boldsymbol{\alpha}) - \rho_1(\boldsymbol{\alpha})\right) \left(\varphi_{\boldsymbol{k}}(\boldsymbol{\alpha}) \cdot \boldsymbol{d}_{1,2}\right)^2 d\boldsymbol{\alpha}^3} \Big/ \hbar,$$

which is of crucial importance in describing the strength of the interaction between metamaterial and quantum dots. $\varphi_{\boldsymbol{k}}(\boldsymbol{\alpha})$ is the eigenstate of the excitation corresponding to the electric field distribution with the energy normalized to $\hbar\omega_{\boldsymbol{k}}/2$, with $\boldsymbol{\alpha}$ being the position of the quantum dot in the unit cell. ρ_2 and ρ_1 are the population densities of the two levels. The transition operators $\hat{\sigma}_{\boldsymbol{k}}^{+}$ and $\hat{\sigma}_{\boldsymbol{k}}^{-}$ indicate the creating and annihilating, respectively, of the quantum dots belonging to the whole system with momentum $\hbar\boldsymbol{k}$ [21]. The rotating wave approximation is used to eliminate the energy non-conserving terms. Considering the maximum population inversion, we have $\rho_2 - \rho_1 \approx \rho$; where $\rho = \rho_2 + \rho_1$ is proportional to r^{-3}. Here, we took a moderate choice on the radius of the quantum dot as $r \approx 2.5$ nm. The dipole moment was chosen to be $|\boldsymbol{d}| = 1.9 \times 10^{-17}$ esu [12]. Then the coupling constant can be calculated [21].

From the interaction Hamiltonian and coupling constant $\mathbf{G}_{\boldsymbol{k}}$, the coupled kinetic equation for the emission processes of quasi-particles of CMP can be obtained. Under strong optical pumped or electric pumped conditions, the energy absorbed by the quantum dots is very large and saturated, and the number of exciton is quite large. We could assume that the number of exciton does not change, $\dot{\hat{\sigma}}_{\boldsymbol{k}}^{z} \approx 0$ and only consider the change of quasi-particles of coupled metamaterial. Additionally, since the homogeneous broadening of the quantum dot spectrum is much narrower than excitation in coupled metamaterial [22], it is considered as a continuous radiation field and a narrow quantum-dot spectral case. Therefore, the stimulated emission rate must be integrated in a narrow frequency range, and the density of the state must be considered. Finally, a stimulated emission rate $\mathcal{B}$ was obtained as $2|\mathbf{G}_{\boldsymbol{k}}|^2 M d/v_g$, which is consistent with the results of Fermi's golden rule (see Appendix A). In this equation, M is the total number of unit cells and v_g is the group velocity derived from the dispersion relation obtained above. Meanwhile, the damping term κ can be considered as $\kappa = \gamma_{meta}$, where $\gamma_{meta} = 1/\tau_{meta}$ represents the decay rate. The stimulated emission coefficient and lifetime of quasi-particle of coupled metamaterial in both systems with different spacing are plotted in Figs. 5a and 5b. When the spacing increases, the coupling between the unit cells decreases as well as lifetime. From Figs. 5a and 5b, we can see that the stimulated emission coefficients in both cases were reduced along with the increase in spacing. With the larger number of available quantum dots, the interaction in Case II became stronger than that in Case I, leading to a larger $\mathcal{B}$. The gain of the system is defined as $\Gamma = \mathcal{B}/\kappa - 1$. Therefore, the cases with $\Gamma > 0$ corresponds to the amplification

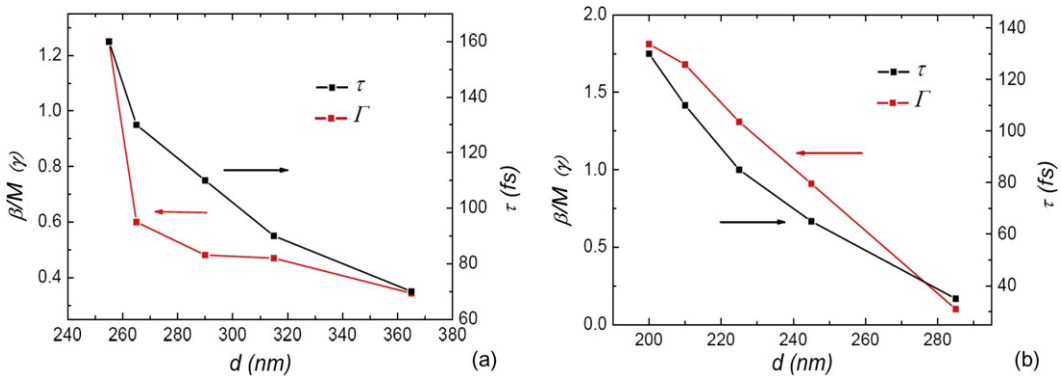

Fig. 5. The stimulated emission coefficient and life time of quasi-particle of CMP in Case I and Case II with different spacing are respectively plotted in (a) and (b).

condition. Furthermore, the stimulated emission coefficient $\mathcal{B}$ is dependent on the number of unit cells according to its expression. Thus, increasing M can further enlarge the stimulated emission. When M is large, $\Gamma > 0$ could be easily obtained, and the amplification by stimulated emission radiation occurs.

5. Conclusion

In summary, we have designed an active system composed of a coupled metamaterial and quantum dot material. The CMP modes have been calculated in this coupled metamaterial in the linear case. A quantum treatment on these CMP modes is developed that enables us to obtain the interaction Hamiltonian of the active system, and the stimulated emission of the CMP is also investigated. The CMP amplification through the stimulated emission radiation is found with a proper choice of the parameters, which is useful in fabrication a CMP source. These results can be used to treat the quantum properties of the coupled metamaterials that may be the future interest, whose counterpart in plasmonic systems has been investigated recently [23,24]. And the quantum efficiency of the nano-lasers, LEDs, and solar cells also need a full quantum theory. It should also be mentioned that the screening and Coulomb interactions in the system have not been considered. These interactions may present interesting effects under certain conditions, which would be further investigated.

Acknowledgements

This work is supported by the State Key Program for Basic Research of China (Nos. 2012CB921501 and 2010CB630703) and the National Natural Science Foundation of China (Nos. 11021403 and 51001059).

Appendix A. Interaction between coupled metamaterial and quantum dot material

The interaction Hamiltonian of the compound system composed of metamaterial and quantum dot material has the following form

$$\mathcal{H}_{Int} = \sum_r -e\boldsymbol{d}(\boldsymbol{r})\cdot\boldsymbol{E}(\boldsymbol{r}), \tag{A.1}$$

where e is the electron charge, $\boldsymbol{d}$ is electric dipole moment of a quantum dot. The summation corresponds to all the quantum dots in the system.

We write the spatial electric field distribution of photon in the mth unit cell as

$$\boldsymbol{E}(\boldsymbol{r}) = \boldsymbol{E}(\boldsymbol{R}_m) = \frac{1}{\sqrt{V}}\int \boldsymbol{E}_{\boldsymbol{K}} e^{i\boldsymbol{K}\cdot\boldsymbol{r}} d\boldsymbol{K} = \frac{1}{\sqrt{M}}\sum_{\boldsymbol{k}+\boldsymbol{G}} \boldsymbol{E}_{\boldsymbol{k}+\boldsymbol{G}} e^{i(\boldsymbol{k}+\boldsymbol{G})\cdot\boldsymbol{R}_m}$$
$$= \frac{1}{\sqrt{M}}\sum_{\boldsymbol{k}}\left(\sum_{\boldsymbol{G}} \boldsymbol{E}_{\boldsymbol{k}+\boldsymbol{G}} e^{i(\boldsymbol{k}+\boldsymbol{G})\boldsymbol{\alpha}}\right) e^{i\boldsymbol{k}\cdot\boldsymbol{R}_m}$$
$$= \frac{1}{\sqrt{M}}\sum_{\boldsymbol{k}} \boldsymbol{E}_{\boldsymbol{k}}(\boldsymbol{\alpha}) e^{i\boldsymbol{k}\cdot\boldsymbol{R}_m} \tag{A.2}$$

where $\boldsymbol{R}_m$ and $\boldsymbol{\alpha}$ denote the center position of the mth unit cell and the location of the quantum dot in this unit cell; $\boldsymbol{K} = \boldsymbol{k} + \boldsymbol{G}$, $\boldsymbol{K}$ is the wave vector of EM wave, $\boldsymbol{k}$ and $\boldsymbol{G}$ are the wave vector in the first Brillouin zone and the reciprocal lattice vector, and M is the total number of unit cells. $\boldsymbol{E}_{\boldsymbol{k}}(\boldsymbol{\alpha})$ corresponds to the electric field distribution of the unit cell with wave vector $\boldsymbol{k}$.

The quantized electric field can be expressed as

$$\boldsymbol{E}(\boldsymbol{r}) = \boldsymbol{E}(\boldsymbol{R}_m + \boldsymbol{\alpha})$$
$$= \frac{1}{\sqrt{M}}\sum_{\boldsymbol{k}} \varphi_{\boldsymbol{k}}(\boldsymbol{\alpha})\left(\hat{a}_{\boldsymbol{k}} e^{i\boldsymbol{k}\boldsymbol{R}_m} + \hat{a}^{+}_{\boldsymbol{k}} e^{-i\boldsymbol{k}\boldsymbol{R}_m}\right). \tag{A.3}$$

Here, $\varphi_{\boldsymbol{k}}(\boldsymbol{\alpha})$ is the normalized electric field distribution with total energy of the unit cell normalized to $\hbar\omega_{\boldsymbol{k}}/2$. The correction of this expression can be proved by substituting (A.3) into $\mathcal{H} = \int(\varepsilon_0(d(\varepsilon\omega)/d\omega)|\boldsymbol{E}(\boldsymbol{r})|^2 + \mu_0|\boldsymbol{H}(\boldsymbol{r})|^2)\,d\boldsymbol{r}/2$, where the magnetic field distribution $\boldsymbol{H}(\boldsymbol{r})$ has the similar form as $\boldsymbol{E}(\boldsymbol{r})$ with the normalized field distribution wrote as $\psi_{\boldsymbol{k}}(\boldsymbol{\alpha})$. After some derivation, we can finally get the Hamiltonian as Eq. (3) in the main text.

The electric dipole moment can be written as $-e\boldsymbol{d}(\boldsymbol{r}) = -e\boldsymbol{d}(\boldsymbol{R}_m + \boldsymbol{\alpha}) = \sum_{\varsigma,\xi}\hat{\sigma}^{m,\boldsymbol{\alpha}}_{\varsigma,\xi}\boldsymbol{d}_{\varsigma,\xi}$, in which ς and ξ denote two levels of the exciton in the quantum dot. Substituting (A.3) into (A.1), we get

$$\hat{\mathcal{H}}_{Int} = \frac{1}{\sqrt{M}}\sum_{\boldsymbol{k}}\sum_{m}\sum_{\boldsymbol{\alpha}}\sum_{\varsigma,\xi}\hat{\sigma}^{m,\boldsymbol{\alpha}}_{\varsigma,\xi}\boldsymbol{d}_{\varsigma,\xi}\cdot\varphi_{\boldsymbol{k}}(\boldsymbol{\alpha})$$
$$\times\left(\hat{a}_{\boldsymbol{k}} e^{i\boldsymbol{k}\boldsymbol{R}_m} + \hat{a}^{+}_{\boldsymbol{k}} e^{-i\boldsymbol{k}\boldsymbol{R}_m}\right). \tag{A.4}$$

After using a rotating-wave approximation to get rid of the energy non-conserving terms, we can obtain the interaction Hamiltonian as

$$\hat{\mathcal{H}}_{Int} = \frac{1}{\sqrt{M}}\sum_{\boldsymbol{k}}\sum_{m}\sum_{\boldsymbol{\alpha}}\varphi_{\boldsymbol{k}}(\boldsymbol{\alpha})\cdot\boldsymbol{d}_{1,2}$$
$$\times\left(\hat{a}_{\boldsymbol{k}}\hat{\sigma}^{m,\boldsymbol{\alpha}}_{+} e^{i\boldsymbol{k}\boldsymbol{R}_m} + \hat{a}^{+}_{\boldsymbol{k}}\hat{\sigma}^{m,\boldsymbol{\alpha}}_{-} e^{-i\boldsymbol{k}\boldsymbol{R}_m}\right). \tag{A.5}$$

The summation on $\boldsymbol{\alpha}$ can be converted into an integral in the unit cell, by introducing a coupling constant

$$\boldsymbol{G}_{\boldsymbol{k}} = \sqrt{\int\left(\rho_2(\boldsymbol{\alpha}) - \rho_1(\boldsymbol{\alpha})\right)\left(\varphi_{\boldsymbol{k}}(\boldsymbol{\alpha})\cdot\boldsymbol{d}_{1,2}\right)^2 d\boldsymbol{\alpha}^3}\Big/\hbar, \tag{A.6}$$

where the integral is in the unit cell, $\rho_1(\boldsymbol{\alpha})$ and $\rho_2(\boldsymbol{\alpha})$ are the population of excitons on two levels. Considering the maximum population inversion, we have $\rho_2(\boldsymbol{\alpha}) - \rho_1(\boldsymbol{\alpha}) \approx \rho(\boldsymbol{\alpha})$, with $\rho(\boldsymbol{\alpha})$ being the concentration of quantum dot. A set of transition operators of quantum dots in the mth unit cell,

$$\hat{\sigma}_+^m = \int \frac{\rho(\boldsymbol{\alpha})\varphi_{\boldsymbol{k}}(\boldsymbol{\alpha}) \cdot \boldsymbol{d}_{1,2}^{m,\boldsymbol{\alpha}}}{\sqrt{\int \rho(\boldsymbol{\alpha})(\varphi_{\boldsymbol{k}}(\boldsymbol{\alpha}) \cdot \boldsymbol{d}_{1,2}^{m,\boldsymbol{\alpha}})^2 \, d\boldsymbol{\alpha}^3}} \hat{\sigma}_+^{m,\boldsymbol{\alpha}} \, d\boldsymbol{\alpha}^3, \tag{A.7}$$

$$\hat{\sigma}_-^m = \int \frac{\rho(\boldsymbol{\alpha})\varphi_{\boldsymbol{k}}(\boldsymbol{\alpha}) \cdot \boldsymbol{d}_{1,2}^{m,\boldsymbol{\alpha}}}{\sqrt{\int \rho(\boldsymbol{\alpha})(\varphi_{\boldsymbol{k}}(\boldsymbol{\alpha}) \cdot \boldsymbol{d}_{1,2}^{m,\boldsymbol{\alpha}})^2 \, d\boldsymbol{\alpha}^3}} \hat{\sigma}_-^{m,\boldsymbol{\alpha}} \, d\boldsymbol{\alpha}^3. \tag{A.8}$$

The transition indicating by these operators belong to all quantum dots in the unit cell. Then we can get

$$\hat{\mathcal{H}}_{Int} = \frac{1}{\sqrt{M}} \hbar \sum_{\boldsymbol{k}} \sum_m \mathbf{G}_{\boldsymbol{k}} \left(\hat{a}_{\boldsymbol{k}} \hat{\sigma}_+^m e^{i\boldsymbol{k}\boldsymbol{R}_m} + \hat{a}_{\boldsymbol{k}}^+ \hat{\sigma}_-^m e^{-i\boldsymbol{k}\boldsymbol{R}_m} \right). \tag{A.9}$$

Finally, we introduce a new set of transition operators of the whole system as

$$\hat{\sigma}_{\boldsymbol{k}}^+ = \frac{1}{\sqrt{M}} \sum_m \hat{\sigma}_+^m e^{i\boldsymbol{k}\boldsymbol{R}_m}, \quad \text{and} \quad \hat{\sigma}_{\boldsymbol{k}}^- = \frac{1}{\sqrt{M}} \sum_m \hat{\sigma}_-^m e^{-i\boldsymbol{k}\boldsymbol{R}_m}, \tag{A.10}$$

corresponding to the transition belonging to the quantum dots of the entire quantum dot system. The simple interaction Hamiltonian can be obtained as

$$\hat{\mathcal{H}}_{Int} = \hbar \sum_{\boldsymbol{k}} \mathbf{G}_{\boldsymbol{k}} \left(\hat{a}_{\boldsymbol{k}} \hat{\sigma}_{\boldsymbol{k}}^+ + \hat{a}_{\boldsymbol{k}}^+ \hat{\sigma}_{\boldsymbol{k}}^- \right). \tag{A.11}$$

For the continuous radiation field, narrow quantum dot spectrum and narrow excitation laser spectrum case, $\boldsymbol{\mathcal{B}} = \boldsymbol{\mathcal{B}}_{\boldsymbol{k}} \cdot \boldsymbol{\mathcal{D}}_{\boldsymbol{k}}$, in which $\boldsymbol{\mathcal{D}}_{\boldsymbol{k}} = \frac{Md}{\pi v_g}$ is the density of state, with d being the spacing between unit cell, and v_g corresponding to the group velocity of this one-dimensional system with wave vector $\boldsymbol{k}$. Since the broadening of quantum dot spectrum have the form:

$$\tilde{g}(\nu, \nu_0) = \frac{\frac{\Delta\nu}{2\pi}}{(\nu - \nu_0)^2 + (\frac{\Delta\nu}{2})^2}, \tag{A.12}$$

with $\Delta\nu = \gamma/\pi, \gamma$ being the damping of the quantum dot, and $\tilde{g}(\nu_0) = 2/\gamma$ in $\boldsymbol{\mathcal{B}}_{\boldsymbol{k}} = |\mathbf{G}_{\boldsymbol{k}}|^2 \tilde{g}(\nu, \nu_0)$.

After the integration with frequency, we have $\boldsymbol{\mathcal{B}} = 2\pi |\mathbf{G}_{\boldsymbol{k}}|^2 \boldsymbol{\mathcal{D}}_{\boldsymbol{k}}$, which is consistent with the Einstein relation. Inserting the density of state in one-dimensional chain, we have

$$\boldsymbol{\mathcal{B}} = 2|\mathbf{G}_{\boldsymbol{k}}|^2 \frac{Md}{v_g}. \tag{A.13}$$

References

[1] J.B. Pendry, A.J. Holden, D.J. Robbins, W.J. Stewart, IEEE Trans. Microwave Theory Tech. 47 (1999) 2075.
[2] N. Engheta, Science 317 (2007) 1698.
[3] H. Liu, et al., Phys. Rev. B 76 (2007) 073101.
[4] N. Liu, H. Liu, S.N. Zhu, H. Giessen, Nature Photonics 3 (2009) 157;
S. Zhang, D.A. Genov, Y. Wang, M. Liu, X. Zhang, Phys. Rev. Lett. 101 (2008) 047401.
[5] R.A. Shelby, D.R. Smith, S. Schultz, Science 292 (2001) 77;
N. Fang, H. Lee, C. Sun, X. Zhang, Science 208 (2005) 534.
[6] J.B. Pendry, D. Schurig, D.R. Smith, Science 312 (2006) 1780.
[7] Y. Lai, et al., Phys. Rev. Lett. 102 (2009) 253902.
[8] H. Liu, et al., Phys. Rev. Lett. 97 (2006) 243902.
[9] Jason Valentine, Shuang Zhang, Thomas Zentgraf, et al., Nature 455 (2008) 376.
[10] David Pines, Elementary Exictations in Solids, Westview Press, 1999.
[11] L.D. Landau, Soviet Phys. JETP 3 (1957) 920.
[12] D.J. Bergman, M.I. Stockman, Phys. Rev. Lett. 90 (2003) 27402;
M.I. Stockman, J. Opt. 12 (2010) 024004.
[13] N.I. Zheludev, et al., Nature Photonics 2 (2008) 351.
[14] E. Altewischer, M.P. van Exter, J.P. Woerdman, Nature 418 (2002) 304;
A. Huck, et al., Phys. Rev. Lett. 102 (2009) 246802.
[15] D.E. Chang, A.S. Sorensen, P.R. Hemmer, M.D. Lukin, Phys. Rev. Lett. 97 (2006) 053002;
A.V. Akimov, et al., Nature 450 (2007) 402;
A.L. Falk, et al., Nature Phys. 5 (2009) 475;
M.S. Tame, et al., Phys. Rev. Lett. 101 (2008) 190504;
D. Ballester, M.S. Tame, C. Lee, J. Lee, M.S. Kim, Phys. Rev. A 79 (2009) 053845.
[16] S. Zhang, et al., Opt. Express 14 (2006) 6778;
S. Linden, et al., Science 306 (2004) 1351.
[17] S.M. Wang, T. Li, H. Liu, F.M. Wang, et al., Opt. Express 16 (2008) 3560.
[18] C. Kittel, Introduction to Solid State Physics, John Wiley & Sons, New York, 2004.
[19] J. Callaway, Quantum Theory of the Solid State, Academic Press, New York, 1976.
[20] M.S. Tame, C. Lee, J. Lee, D. Ballester, et al., Phys. Rev. Lett. 101 (2008) 190504;
D. Ballester, M.S. Tame, C. Lee, J. Lee, M.S. Kim, Phys. Rev. A 79 (2009) 053845.
[21] Marlan O. Scully, M. Suhail Zubairy, Quantum Optics, Cambridge University Press, 1997.
[22] V.I. Klimov, A.A. Mikhailovsky, S. Xu, A. Malko, et al., Science 290 (2000) 314.
[23] E. Altewischer, M.P. van Exter, J.P. Woerdman, Nature 418 (2002) 304;
A. Huck, S. Smolka, P. Lodahl, A.S. Sørensen, et al., Phys. Rev. Lett. 102 (2009) 246802.
[24] D.E. Chang, A.S. Sorensen, P.R. Hemmer, M.D. Lukin, Phys. Rev. Lett. 97 (2006) 053002;
A.V. Akimov, A. Mukherjee, C.L. Yu, D.E. Chang, et al., Nature 450 (2007) 402;
A.L. Falk, F.H.L. Koppens, C.L. Yu, K. Kang, et al., Nature Phys. 5 (2009) 475.